nature neuroscience

Astrocytes regulate adult hippocampal neurogenesis through ephrin-B signaling

Randolph S Ashton[1,3,4], Anthony Conway[1,4], Chinmay Pangarkar[2], Jamie Bergen[1], Kwang-Il Lim[1,3], Priya Shah[1], Mina Bissell[2] & David V Schaffer[1]

Neurogenesis in the adult hippocampus involves activation of quiescent neural stem cells (NSCs) to yield transiently amplifying NSCs, progenitors, and, ultimately, neurons that affect learning and memory. This process is tightly controlled by microenvironmental cues, although a few endogenous factors are known to regulate neuronal differentiation. Astrocytes have been implicated, but their role in juxtacrine (that is, cell-cell contact dependent) signaling in NSC niches has not been investigated. We found that ephrin-B2 presented from rodent hippocampal astrocytes regulated neurogenesis *in vivo*. Furthermore, clonal analysis in NSC fate-mapping studies revealed a previously unknown role for ephrin-B2 in instructing neuronal differentiation. In addition, ephrin-B2 signaling, transduced by EphB4 receptors on NSCs, activated β-catenin *in vitro* and *in vivo* independently of Wnt signaling and upregulated proneural transcription factors. Ephrin-B2$^+$ astrocytes therefore promote neuronal differentiation of adult NSCs through juxtacrine signaling, findings that advance our understanding of adult neurogenesis and may have future regenerative medicine implications.

In the mammalian brain, neurogenesis persists throughout adulthood in the subgranular zone (SGZ) of the hippocampal dentate gyrus[1] and the subventricular zone (SVZ) of the lateral ventricles[2]. In these niches, neural stem cell (NSC) maintenance, proliferation, and differentiation are orchestrated by a delicate balance of microenvironmental cues. The importance of such instructive signals in the niche is supported by the absence of significant neurogenesis in the adult mammalian CNS outside of these regions[3,4] and by the development of aberrant neurogenesis in patients with pathologies that disrupt the natural chemistry of the brain, for example epilepsy[5], inflammation[6], and neurodegenerative diseases[7].

In the SGZ, adult neurogenesis entails the activation of quiescent type 1 NSCs to produce mitotic, multipotent type 2a NSCs[8,9]; the differentiation of the type 2a NSCs to lineage-committed, proliferative type 2b neuronal precursors and subsequently type 3 neuroblasts; and the survival, migration, and maturation of neuroblasts as they differentiate into granule cells that synaptically integrate into the existing neural network[8–10]. Each of these stages is regulated by signals within the niche. For example, bone morphogenic protein[11] and Notch[12,13] signaling modulate the balance between quiescent and proliferative NSCs, and Sonic hedgehog[14], fibroblast growth factor-2 (ref. 15), vascular endothelial growth factor[16] and Wnt7a[17] regulate NSC proliferation.

Although there is increasing knowledge of niche factors that regulate NSC division, substantially less is known about key signals that instruct cells in the SGZ to undergo neuronal differentiation[18,19]. GABA inputs from local neuronal circuitry[20] and systemic retinoic acid levels[21] modulate NSC neuronal fate commitment. Furthermore, while neuronal differentiation precedes gliogenesis during CNS development, adult hippocampal astrocytes directly induce neuronal differentiation of NSCs *in vitro* via both secreted and membrane-associated factors[22], and the former have since been found to include Wnt3a[23] and potentially additional secreted signals[19]. However, the membrane-bound astrocytic components[22] that may be critical for neuronal fate commitment *in vivo* remain unknown.

Ephrins are a diverse class of glycophosphatidylinositol-linked (ephrinA1–6) and transmembrane (ephrinB1–3) cell surface ligands that bind Eph receptors (EphA1–10 and EphB1–6) on opposing cell membranes to initiate bidirectional signaling[24]. Ephrin-Eph signaling is traditionally known to control the spatial organization of cells and their projections by modulating intercellular attractive and repulsive forces[25]. For example, ephrin-Eph signaling instructs topographical mapping of hippocampo-septal and entorhino-hippocampal projections during development[26] and regulates neuronal dendrite spine morphogenesis and synaptogenesis of adult hippocampal neurons[27].

Recent studies have also indicated that ephrin-Eph signaling has an earlier role in regulating stem cell behavior. For example, ephrin-A–EphA signaling promotes embryonic telencephalic NSC differentiation[28], and ephrin-B3–EphB3 signaling may exert an anti-proliferative effect on NSCs in the developing SVZ[29]. In the adult CNS, infusion of ephrin-B2 or EphB2 ectodomains into the lateral ventricles induced SVZ NSC proliferation and disrupted neuroblast migration through the rostral migratory stream[30]. In addition, signaling between ephrin-A2$^+$ neural stem cells, and EphA7$^+$ ependymal cells and putative stem cells,

[1]Department of Chemical and Biomolecular Engineering, University of California Berkeley, Berkeley, California, USA. [2]Life Sciences Division, Lawrence Berkeley National Laboratory, Berkeley, California, USA. [3]Present address: Department of Biomedical Engineering, Wisconsin Institutes for Discovery, University of Wisconsin Madison, Madison, Wisconsin, USA (R.S.A.), Department of Medical and Pharmaceutical Sciences, College of Science, Sookmyung Women's University, Seoul, Korea (K.-I.L.). [4]These authors contributed equally to this work. Correspondence should be addressed to D.V.S. (schaffer@berkeley.edu).

Received 22 May; accepted 9 August; published online 16 September 2012; doi:10.1038/nn.3212

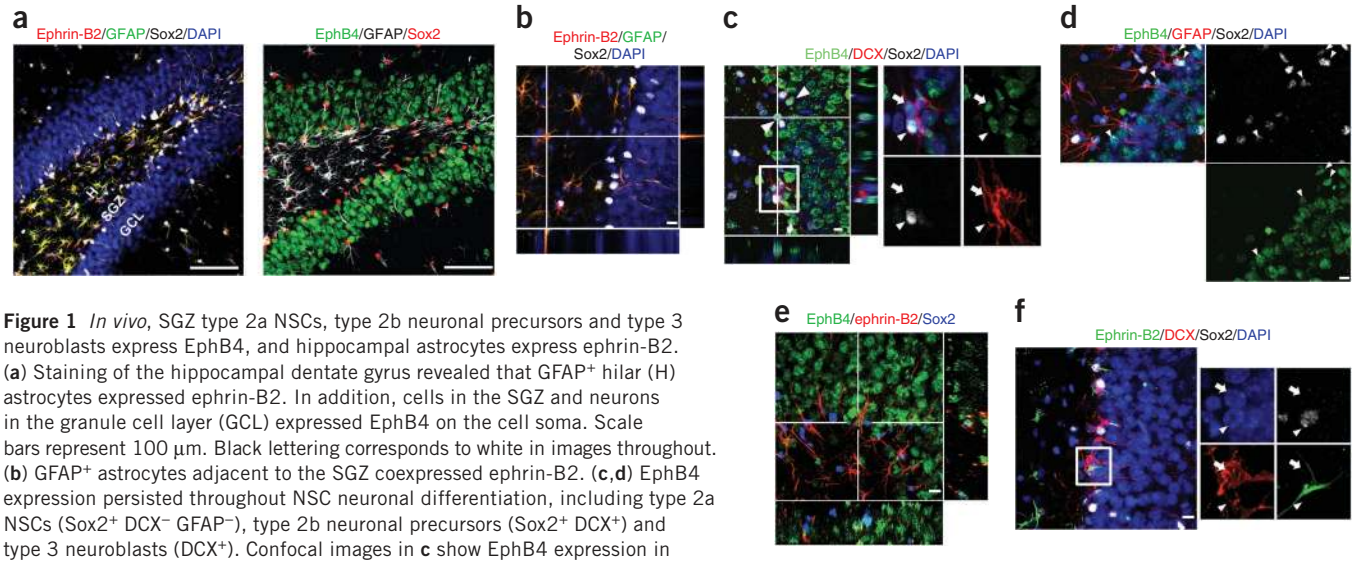

Figure 1 *In vivo*, SGZ type 2a NSCs, type 2b neuronal precursors and type 3 neuroblasts express EphB4, and hippocampal astrocytes express ephrin-B2. (**a**) Staining of the hippocampal dentate gyrus revealed that GFAP$^+$ hilar (H) astrocytes expressed ephrin-B2. In addition, cells in the SGZ and neurons in the granule cell layer (GCL) expressed EphB4 on the cell soma. Scale bars represent 100 μm. Black lettering corresponds to white in images throughout. (**b**) GFAP$^+$ astrocytes adjacent to the SGZ coexpressed ephrin-B2. (**c**,**d**) EphB4 expression persisted throughout NSC neuronal differentiation, including type 2a NSCs (Sox2$^+$ DCX$^-$ GFAP$^-$), type 2b neuronal precursors (Sox2$^+$ DCX$^+$) and type 3 neuroblasts (DCX$^+$). Confocal images in **c** show EphB4 expression in Sox2$^+$ DCX$^-$ cells (large arrowheads) in the SGZ. The magnified region depicts the presence of EphB4 expression on a Sox2$^+$ DCX$^+$ type 2b neuronal precursor (small arrowheads) and a DCX$^+$ type 3 neuroblast (arrows). Confocal images in **d** show EphB4 expression by Sox2$^+$ GFAP$^-$ cells (small arrowheads); thus, Sox2$^+$ DCX$^-$ GFAP$^-$ type 2a NSCs also expressed EphB4. (**e**,**f**) Given the close proximity of ephrin-B2$^+$ astrocytes to EphB4$^+$ cells in the SGZ, ephrin-B2–EphB4 juxtacrine signaling is in a position to induce NSC differentiation into Sox2$^+$ DCX$^+$ type 2b neuronal precursors (small arrowheads) and subsequently Sox2$^-$ DCX$^+$ type 3 neuroblasts (arrows). The scale bars represent 10 μm (**b**–**f**). Crosshairs represent the position of *x-z* (right panel) and *y-z* (bottom panel) orthogonal slices of the confocal stack depicted in the image (**b**,**d**,**e**).

was shown to suppress proliferation of NSCs in the adult SVZ[31]. In the adult SGZ, ephrin-B3$^+$ neurons in the granule cell layer have been proposed to regulate EphB1$^+$ NSC polarity, SGZ positioning, and proliferation[32]. Similarly, in *Efna5*$^{-/-}$ mice, a decrease in both the proliferation of NSCs and the survival and maturation of newborn neurons in the adult SGZ was observed[33]. Thus, ephrin-Eph signaling has been shown to affect the proliferation, migration and survival of adult NSCs; however, its potential regulation of NSC fate commitment remains unknown.

We found that ephrin-B2 presented by hippocampal astrocytes instructed neuronal differentiation of NSCs in the SGZ of the adult hippocampus. Furthermore, ephrin-B2–EphB4 forward signaling induced neuronal differentiation of NSCs by activating β-catenin, independent of Wnt signaling, and inducing transcription of proneural transcription factors. Our findings describe a juxtacrine signaling mechanism by which astrocytes actively regulate neuronal differentiation of NSCs during adult neurogenesis.

RESULTS

Ephrin-B2 and EphB4 expression in the SGZ

In the SGZ, type 1 NSCs express the SRY-box 2 (Sox2) transcription factor and stain for glial fibrilary acid protein (GFAP) and Nestin along radial granule cell layer (GCL)-spanning or horizontal processes[13]. Type 2a NSCs[9] remain Sox2$^+$ and Nestin$^+$, but downregulate GFAP expression, and fate-restricted, proliferative type 2b neuronal precursors coexpress Sox2 and doublecortin (DCX) while downregulating Nestin expression. The latter then mature into (Sox2$^-$ DCX$^+$) type 3 neuroblasts, which migrate into the GCL and become neuronal-specific nuclear protein (NeuN)$^+$ DCX$^-$ granule neurons[8,10,11,13]. Alternatively, type 1 NSCs can differentiate into stellate, Sox2$^-$ GFAP$^+$ hippocampal astrocytes, which are primarily located in the hilus adjacent to the SGZ[10].

As part of a candidate screen, we investigated ephrin-B2 expression in the hippocampal dentate gyrus. Antibody to Ephrin-B2 consistently labeled GFAP$^+$ astrocytes in the hilus, SGZ and molecular layer (**Fig. 1a**,**b**). In contrast, EphB4, an ephrin-B2 receptor, was expressed by Sox2$^+$ DCX$^-$, Sox2$^+$ DCX$^+$, Sox2$^-$ DCX$^+$ and Sox2$^+$ GFAP$^-$ cells in the SGZ, as well as by the majority of cells in the GCL (**Fig. 1a**,**c**,**d**). Thus, EphB4 appeared to be expressed in type 2a (Sox2$^+$ DCX$^-$ GFAP$^-$) NSCs and persisted as these cells became type 2b neuronal precursors (Sox2$^+$ DCX$^+$), type 3 neuroblasts (Sox2$^-$ DCX$^+$) and eventually granule neurons. Some type 1 NSCs were EphB4$^+$, although EphB4 was not expressed at levels detectable by immunostaining in many cells (data not shown). Overall, these results indicate that astrocytes are a source of ephrin-B2 ligand in the dentate gyrus and suggest that EphB4-expressing NSCs, neuronal precursors and neuroblasts contact these ligand-expressing astrocytes (**Fig. 1e**,**f**).

Ephrin-B2 increases neurogenesis *in vitro* and *in vivo*

Ephrin-Eph signaling begins with clustering of multiple ligand-receptor complexes at sites of cell-cell contact[24]. Thus, to initially explore a possible role for ephrin-B2 in regulating NSC fate, we added antibody-clustered ephrin-B2–Fc fusion molecules (Fc–ephrin-B2)[34] to adult hippocampus–derived NSCs in culture and found that they induced a strong, dose-dependent increase in NSC neuronal differentiation (**Fig. 2a**,**b**). No biological activity was observed with monomeric, unclustered ephrin-B2 and Fc, consistent with previous findings[30,34], and no proliferative effect was observed under any conditions (data not shown). To investigate which receptor mediated Fc–ephrin-B2's activity, we pre-incubated the NSCs with an antibody to either EphB2 or EphB4, two known ephrin-B2 receptors, before adding Fc–ephrin-B2. Inhibition of EphB4, but not EphB2, significantly reduced Fc–ephrin-B2 induction of neuronal differentiation ($P = 0.002$; **Fig. 2c**), indicating that EphB4 receptors mediate the proneuronal effect of Fc–ephrin-B2. Reverse transcription PCR (RT-PCR) and immunocytochemistry results confirmed that hippocampus-derived NSCs express EphB4 (**Fig. 2d**), in contrast with SVZ NSCs, which reportedly do not express this receptor (ref. 30).

Given our staining and *in vitro* results, we hypothesized that astrocytic ephrin-B2 actively promotes neuronal differentiation of NSCs

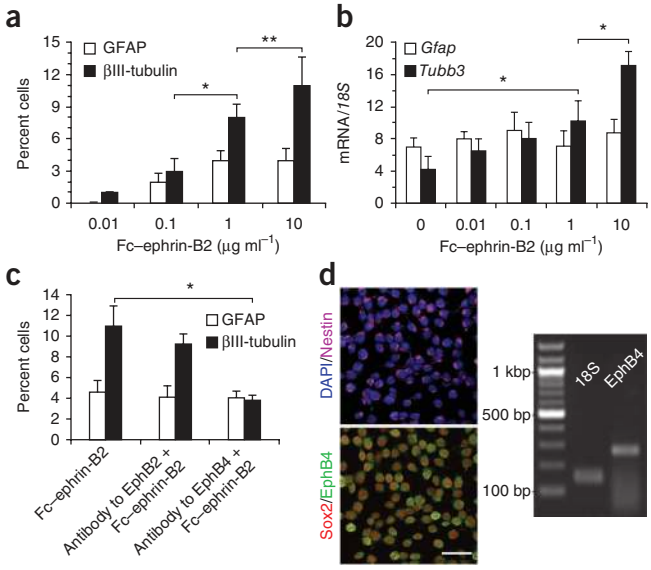

Figure 2 Fc–ephrin-B2 promoted the neuronal differentiation of NSCs *in vitro*. (**a**,**b**) Stimulation by Fc–ephrin-B2 induced NSCs to undergo neuronal differentiation (βIII-tubulin$^+$ or *Tubb3*) in a dose-responsive fashion, as measured by immunocytochemistry and QPCR ($n = 3$, experimental replicates). GFAP staining was slightly increased with ephrin-B2, but no increase in expression was observed by QPCR. (**c**) Blockage of the ephrin-B2 receptors EphB2 and EphB4 during Fc–ephrin-B2 (10 μg ml^{-1}) stimulation revealed that EphB4 mediates Fc–ephrin-B2's proneuronal effect on NSCs ($n = 3$, experimental replicates). ANOVA and a multi-variable Tukey-Kramer analysis was conducted, $^*P < 0.01$ and $^{**}P < 0.05$. Data are represented as means ± s.d. (**d**) Nestin$^+$ Sox2$^+$ NSCs expressed EphB4, as seen by immunocytochemistry and RT-PCR. Scale bar represents 100 μm.

in the SGZ through juxtacrine signaling, and therefore proceeded to investigate Fc–ephrin-B2 activity *in vivo* (**Fig. 3**). Mitotic cells in the brain of adult rats were first labeled with BrdU, followed by bilateral hippocampal injections of phosphate-buffered saline (PBS), nonclustered ephrin-B2, antibody to Fc without ephrin-B2, or Fc–ephrin-B2 (**Fig. 3a**). Histology revealed an increase in the number of BrdU$^+$ cells in the SGZ of rats injected with Fc–ephrin-B2 compared with rats treated with vehicle or clustering antibody controls 5 d after injection (**Fig. 3c**), mirroring one report in the SVZ[30]. In addition, no difference in the percentage of BrdU$^+$ cells that co-stained as nonradial GFAP$^+$ astrocytes was observed between experimental groups on day 5 (**Supplementary Fig. 1a**,**b**). However, there was a considerable increase in the proportion of BrdU$^+$ cells that co-stained for DCX in animals injected with Fc–ephrin-B2 (80.6 ± 0.87%) as compared with those injected with PBS (40.65 ± 4.15%), ephrin-B2 (50.3 ± 3.45%) or antibody to Fc (50.37 ± 9.28%) (**Fig. 3b**,**d**). These results indicate that ephrin-B2 signaling *in vivo* may regulate early stages of adult hippocampal neurogenesis by modulating NSC proliferation and/or differentiation, but further analysis is required to distinguish between these two possibilities.

Astroctyic ephrin-B2 regulates neurogenesis *in vitro*

Exogenous ephrin-B2 elevates hippocampal neurogenesis, and astrocytes expressing ephrin-B2 contact NSCs in the hippocampus; however, it remains unclear whether astrocytic ephrin-B2 regulates NSC fate. Previous studies have found that hippocampal astrocytes promote neuronal differentiation of co-cultured NSCs through secretion of soluble Wnt3a and by unidentified membrane-bound signaling molecules[22,23]. To determine whether ephrin-B2 is an important component of this membrane-associated activity, we first verified its expression in cultured hippocampal astrocytes. Consistent with our *in vivo* results (**Fig. 1**), quantitative PCR (QPCR) revealed that hippocampus-derived astrocytes express *Efnb2* mRNA at levels three orders of magnitude higher than cultured NSCs (**Supplementary Fig. 2a**). Notably, cultured NSCs downregulated EphB4 and upregulated ephrin-B2 expression following astrocytic differentiation, yet maintained EphB4 expression on their soma following neuronal differentiation into DCX$^+$ immature neurons (**Supplementary Fig. 2b**).

We then analyzed whether RNAi-mediated knockdown of ephrin-B2 in hippocampal astrocytes could compromise their ability to induce neuronal differentiation of NSCs in co-culture. We screened five candidate *Efnb2* short hairpin RNA (shRNA) sequences expressed under a human and/or a mouse U6 promoter upstream of a *UBC* promoter–eGFP expression cassette (**Supplementary Fig. 3**). Following lentiviral delivery, QPCR analysis revealed that two shRNA constructs (*Efnb2* shRNA #1 and #2) could knock down *Efnb2* mRNA levels in astrocytes by approximately 90 and 85%, respectively (**Fig. 4a**). Next, BrdU-labeled NSCs (>95%) were seeded on near-confluent layers of mitotically inactive astrocytes that were either naive or expressing *Efnb2* shRNA #1 or #2, or *lacZ* shRNA, and the co-cultures were immunostained after 6 d. NSC proliferation was minimal in all experimental groups. However, the percentage of βIII-tubulin$^+$ BrdU$^+$ cells increased from 6.79 ± 0.62% in NSC-only control cultures to 14.2 ± 0.55% in NSC and naive astrocyte co-cultures (**Fig. 4b**), levels that are consistent with a prior NSC-astrocyte co-culture study[22], and the neuronally differentiated NSCs were primarily located in close proximity to astrocytes (**Fig. 4c**). A similar proneuronal effect was maintained

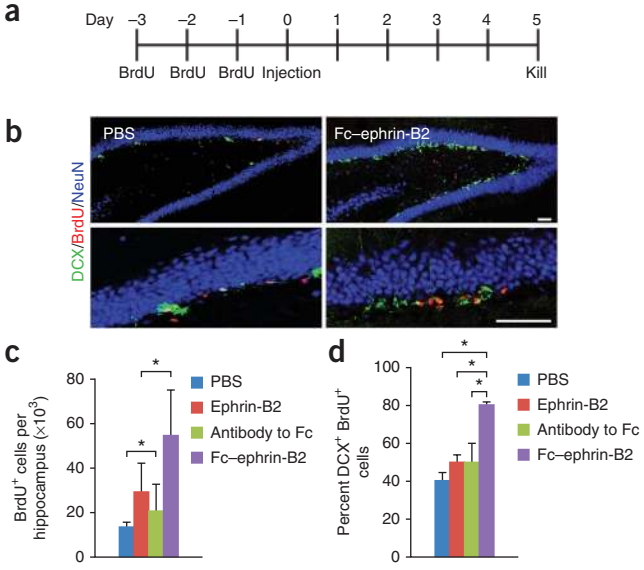

Figure 3 Intrahippocampal injection of Fc–ephrin-B2 increases neurogenesis in the SGZ. (**a**) Schematic of experimental time course. (**b**) Administration of Fc–ephrin-B2 into the hippocampus increased neurogenesis, as shown by representative confocal images of the dentate gyrus and SGZ (close up). The scale bars represent 100 μm. (**c**) Injection of exogenous ephrin-B2 ligands increased BrdU$^+$ cell numbers compared with injection of vehicle and constituent controls. (**d**) Only injection of Fc–ephrin-B2, but not its constituent controls, increased the percentage of BrdU$^+$ cells that co-stained for DCX in the SGZ ($n = 3$ brains, analyzed 8 hippocampal sections per brain). $^*P < 0.01$ and $^{**}P < 0.05$. Error bars represent ± s.d.

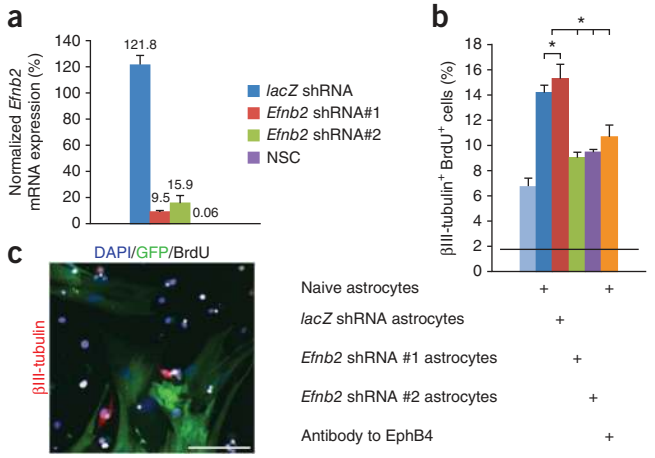

Figure 4 *Efnb2* RNAi decreases the proneuronal effect of hippocampus-derived astrocytes *in vitro*. (**a**) *Efnb2* shRNA lentiviral vectors (#1 and #2) inhibited *Efnb2* expression in hippocampus-derived astrocytes. Expression levels were measured by QPCR and normalized to *Efnb2* expression in non-infected hippocampus-derived astrocytes (that is, 100%). In addition, hippocampus-derived astrocytes expressed orders of magnitude more *Efnb2* than NSCs ($n = 3$, technical replicates). (**b**) Naive astrocytes and astrocytes expressing a control *lacZ* shRNA promoted neuronal differentiation of NSCs compared to NSC-only cultures. However, knockdown of astrocyte *Efnb2* expression, or antibody blockage of NSC EphB4 receptors, significantly diminished the proneuronal effect of hippocampus-derived astrocytes, as seen by the decrease in the percentage of βIII-tubulin$^+$ BrdU$^+$ NSCs to levels closer to those observed in NSC-only cultures ($n = 4$, experimental replicates). The solid black line indicates the level of βIII-tubulin$^+$ BrdU$^+$ cells at the start of the experiment. (**c**) Representative confocal image of NSCs labeled with BrdU (white) differentiated into βIII-tubulin$^+$ neurons after co-culture with lentiviral vector–expressing (that is, GFP$^+$) astrocytes. NSCs adjacent to astrocytes had a higher propensity for neuronal differentiation. Scale bar represents 100 μm. $^*P < 0.01$. Error bars represent ± s.d.

by astrocytes expressing the *lacZ* shRNA (15.4 ± 1.12%); however, knockdown of ephrin-B2 expression in *Efnb2* shRNA #1 and #2 astrocytes decreased their neuronal instructive potential by ~70% (to 9.09 ± 0.39% and 9.51 ± 0.11% βIII-tubulin$^+$ BrdU$^+$ cells, respectively). Notably, this decrease in NSC neuronal differentiation resulting from ephrin-B2 knockdown is comparable to the previously observed ~55% loss when NSCs were cultured in astrocyte-conditioned medium rather than in co-culture[22]. Furthermore, antibody blockage of EphB4 receptors in the co-culture assay also inhibited the proneuronal effect of naive astrocytes, resulting in only 10.75 ± 0.87% of NSCs differentiating into βIII-tubulin$^+$ BrdU$^+$ neurons. Thus, ephrin-B2 is an important membrane-presented factor that hippocampal astrocytes employ to instruct neuronal differentiation of NSCs *in vitro*, and EphB4 receptors on NSCs transduce this signal.

Loss of astrocytic ephrin-B2 decreases neurogenesis in SGZ

To determine whether endogenous ephrin-B2 signaling promotes neuronal differentiation *in vivo*, we injected adult rats intrahippocampally with lentiviral vectors encoding *Efnb2* shRNA #1 or #2, or control *lacZ* shRNA. After 2 weeks, mitotic cells in the SGZ were labeled with BrdU, and tissue samples were collected 5 d later (**Fig. 5a**). In GFP$^+$ regions of the hippocampus, ephrin-B2 levels from rats treated with the *Efnb2* shRNA constructs were markedly lower than in sections from PBS- or *lacZ* shRNA–treated rats, which exhibited ephrin-B2 expression in patterns similar to GFAP staining (**Fig. 5b**). We noted that neurons, rather than astrocytes, expressed GFP in the lentiviral vector–infected hippocampi; however, it was later confirmed through administration of an otherwise identical lentiviral vector in which the *UBC* promoter was replaced with a *Gfap* promoter[22] that the low GFP expression initially observed in astrocytes was a result of the ubiquitin promoter (**Supplementary Fig. 4a**,**b**). In either case, the U6 promoter driving the shRNA expression mediated strong ephrin-B2 knockdown in hippocampal astrocytes (**Fig. 5b** and **Supplementary Fig. 4c**).

Next, BrdU$^+$ and DCX$^+$ BrdU$^+$ cells in the SGZ were quantified in GFP$^+$ hippocampi (**Fig. 5c**). In contrast with results obtained after administration of exogenous ephrin-B2, no significant difference ($P = 0.217$) in the number of BrdU$^+$ cells per mm^3 was observed in rats treated with *Efnb2* shRNA #1 (33.2 ± 11.3%) and #2 (22.5 ± 2.50%) versus *lacZ* shRNA control rats (29.0 ± 7.20%; **Fig. 5d**), indicating that endogenous ephrin-B2 signaling does not by itself regulate the proliferation of NSCs and type 2b neuronal precursors. However, consistent with the proneuronal effect of Fc–ephrin-B2 *in vitro* and *in vivo*, the percentage of BrdU$^+$ cells that co-stained for DCX was significantly lower ($P < 0.001$) in animals treated with *Efnb2* shRNA #1 (32.3 ± 4.95%) and #2 (41.6 ± 3.41%) compared with *lacZ* shRNA (59.4 ± 2.33%; **Fig. 5e**). Thus, knockdown of ephrin-B2 expression in hippocampal astrocytes decreased neurogenesis in the adult SGZ.

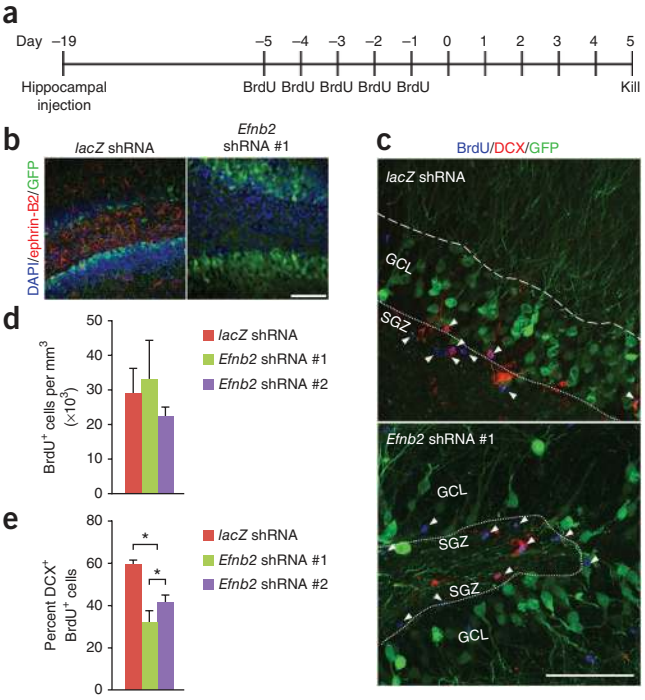

Figure 5 *Efnb2* RNAi decreases neuronal differentiation of BrdU$^+$ cells in the SGZ. (**a**) Schematic of experimental time course. (**b**) Regions of the hippocampus transduced with lentiviral vector (GFP$^+$) carrying *Efnb2* shRNA #1 (and #2; data not shown) showed considerably less ephrin-B2 staining than hippocampi for *lacZ* shRNA lentivirus–injected rats. (**c**) Representative confocal images showing decreased neuronal differentiation, that is, DCX$^+$ co-staining, of BrdU$^+$ (arrowheads) cells in the SGZ of rats injected with lentivirus encoding *Efnb2* shRNA. (**d**,**e**) Knockdown of ephrin-B2 in the hippocampal niche did not affect BrdU$^+$ cell numbers, but it did result in a significant decrease in the percentage of BrdU$^+$ cells that co-stained for DCX in the SGZ ($n = 4$ brains, analyzed 8 hippocampal sections per brain). This suggests that endogenous ephrin-B2 signaling regulates neuronal differentiation of NSCs. $^*P < 0.01$. Error bars represent ± s.d. The dotted line marks the SGZ-hilus boundary and the dashed line marks the GCL-MCL boundary. Scale bars represent 100 μm.

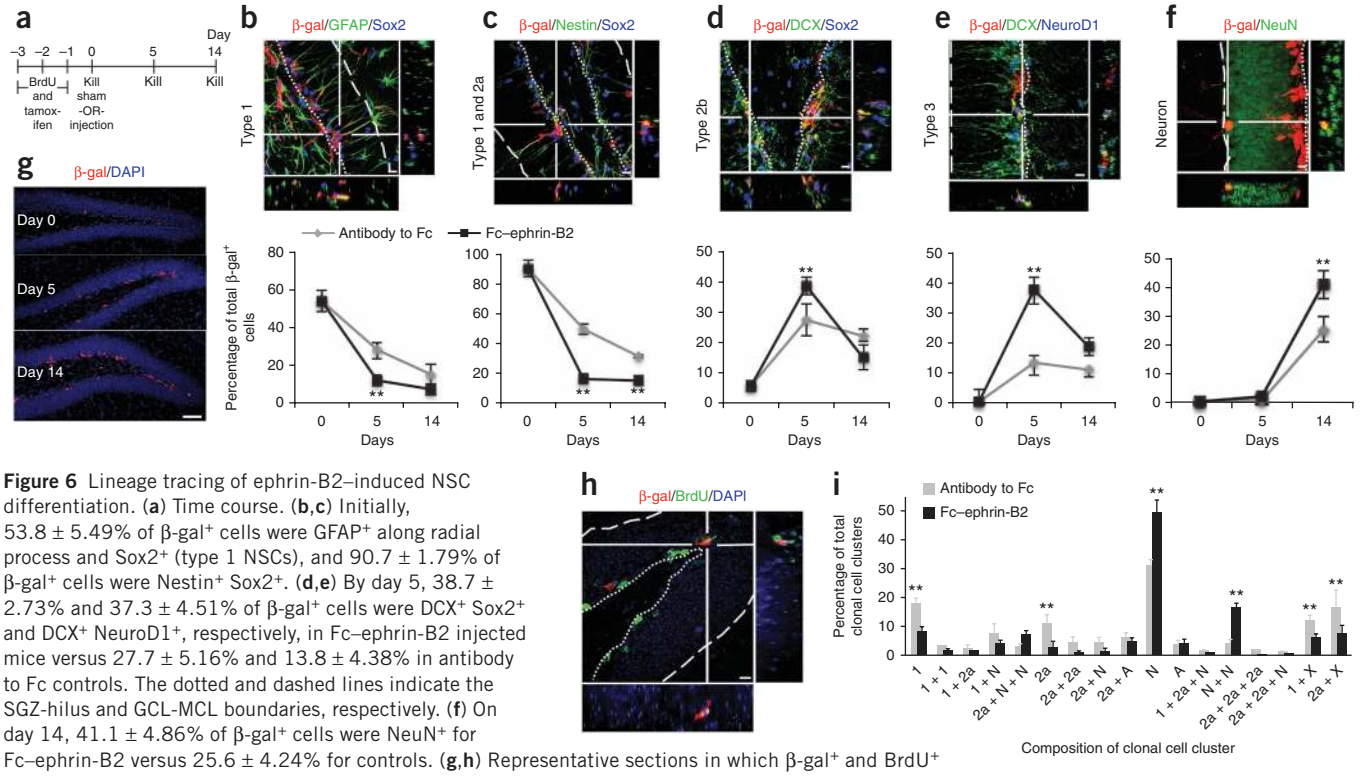

Figure 6 Lineage tracing of ephrin-B2–induced NSC differentiation. (**a**) Time course. (**b**,**c**) Initially, 53.8 ± 5.49% of β-gal$^+$ cells were GFAP$^+$ along radial process and Sox2$^+$ (type 1 NSCs), and 90.7 ± 1.79% of β-gal$^+$ cells were Nestin$^+$ Sox2$^+$. (**d**,**e**) By day 5, 38.7 ± 2.73% and 37.3 ± 4.51% of β-gal$^+$ cells were DCX$^+$ Sox2$^+$ and DCX$^+$ NeuroD1$^+$, respectively, in Fc–ephrin-B2 injected mice versus 27.7 ± 5.16% and 13.8 ± 4.38% in antibody to Fc controls. The dotted and dashed lines indicate the SGZ-hilus and GCL-MCL boundaries, respectively. (**f**) On day 14, 41.1 ± 4.86% of β-gal$^+$ cells were NeuN$^+$ for Fc–ephrin-B2 versus 25.6 ± 4.24% for controls. (**g**,**h**) Representative sections in which β-gal$^+$ and BrdU$^+$ cells proliferated and differentiated over 14 d. (**i**) Compared with antibody to Fc, Fc–ephrin-B2 decreased the number of single type 1 (1, 8.01 ± 1.91% versus 17.8 ± 1.93%) and type 2a NSCs (2a, 2.51 ± 2.34% versus 10.8 ± 3.22%) and increased single neuroblasts or neurons (N, 49.2 ± 4.57% versus 30.9 ± 2.28%). Furthermore, ephrin-B2 decreased the number of doublets containing a type 1 (1 + X, 5.95 ± 1.47% versus 11.8 ± 2.03%) or type 2a (2a + X, 7.37 ± 3.00% versus 16.5 ± 6.03%) cell and increased neuroblasts or neuron doublets (N + N,16.3 ± 1.82% versus 3.87 ± 1.65%). Cluster size (1.55 ± 0.03 versus 1.54 ± 0.04) and overall β-gal$^+$ cell numbers (**Supplementary Fig. 5**) were indistinguishable in Fc–ephrin-B2 versus control mice. Thus, ephrin-B2 signaling increased neuronal differentiation without altering proliferation. $^{**}P < 0.05$. Error bars represent ± s.d. Five sections (ten hemispheres) analyzed in $n = 4$ antibody to Fc–treated and 5 Fc–ephrin-B2–treated brains; dotted and dashed lines indicate SGZ-hilus and GCL-MCL boundaries, respectively. Scale bars represent 10 μm (**b**–**f**,**h**) and 100 μm (**g**).

Ephrin-B2 signaling instructs NSC neuronal differentiation

To gain insight into whether neural stem and/or progenitor cell populations are modulated by ephrin-B2, we developed an inducible, conditional reporter mouse strain to map the fate of Nestin$^+$ NSCs in response to exogenous ephrin-B2. *Nestin-CreER^{T2}* (ref. 35) and *R26-stop$^{loxP/loxP}$-lacZ* (ref. 36) mice were bred to generate mice in which tamoxifen administration induced *lacZ* expression in Nestin$^+$ cells via a transient recombination event. Using adult *Nestin-CreER^{T2}; R26-stop$^{loxP/loxP}$-lacZ* mice, cells were colabeled by BrdU and tamoxifen injections before an intrahippocampal injection of Fc–ephrin-B2 or the Fc antibody control, and tissue sections were collected at day 0 from sham mice and at day 5 and 14 post-treatment (**Fig. 6a**). Quiescent and mitotic cells in the SGZ were labeled β-galactosidase$^+$ (β-gal) and BrdU$^+$ in a near clonal fashion on day 0 (43.6 ± 7.95% of β-gal$^+$ cells were also BrdU$^+$, 3.89 ± 1.00% of BrdU$^+$ cells were also β-gal$^+$), and these cells expanded, differentiated and migrated into the GCL over the 14-d observation period (**Fig. 6b**–**h**). At the population level, β-gal$^+$ hippocampal cells initially (day 0) consisted of type 1 and 2a Nestin$^+$ Sox2$^+$ NSCs (90.7 ± 1.79%), and a large fraction of β-gal$^+$ cells were specifically type 1, radial, GFAP$^+$ Sox2$^+$ NSCs (53.8 ± 5.49%; **Fig. 6b**–**f**). By day 5, the total number of β-gal$^+$ cells had increased, but to the same extent in Fc–ephrin-B2 and Fc control antibody groups (**Supplementary Fig. 5a**). At this time point, however, a larger fraction of the β-gal$^+$ cell population in mice injected with Fc–ephrin-B2 had shifted from type 1 and 2a NSCs to neuronal fate–committed type 2b DCX$^+$ Sox2$^+$ precursors and even more so to type 3 DCX$^+$ NeuroD1$^+$ neuroblasts, as compared with mice injected with Fc control antibody (**Fig. 6d**,**e**). By day 14, the total number of β-gal$^+$ cells was again consistent between experimental groups, but the increase in neuronal-fated β-gal$^+$ cells in mice injected with Fc–ephrin-B2 versus Fc control antibody persisted as type 2b and type 3 cells matured into NeuN$^+$ GCL neurons (**Fig. 6d**–**f** and **Supplementary Fig. 5a**).

To gain further insights into the early fate decisions that ephrin-B2 modulates[10], we analyzed individual β-gal$^+$ cell clusters that were likely clonal. This quantification was conducted at day 5 in Nestin and Sox2 co-stained hippocampal sections (a total of 916 and 1,145 cell clusters were analyzed in $n = 4$ Fc control antibody–treated and 5 Fc–ephrin-B2–treated brains, respectively). Type 1 and type 2a cells were identified by Nestin$^+$ Sox2$^+$ co-staining and distinguished by morphology, and β-gal$^+$ Nestin$^-$ Sox2$^-$ cells were deemed astrocytes or other neuronal cells (presumably neuronal precursors, neuroblasts or mature neurons) by morphology and positioning relative to the GCL (**Fig. 6i**). We observed that the vast majority of clonal β-gal$^+$ cell clusters contained three or fewer cells. Notably, the average number of cells per cluster was 1.55 ± 0.03 and 1.54 ± 0.04 cells in Fc control antibody and Fc–ephrin-B2 sections, respectively, again indicating that Fc–ephrin-B2 did not enhance proliferation of type 1 or type 2a cells, in contrast with the previously observed increase in BrdU$^+$ cells with Fc–ephrin-B2 (**Fig. 3c**). Furthermore, the cell phenotype distribution of the β-gal$^+$ cell clusters mirrored the overall population-level results (**Fig. 6b**–**f** and **Supplementary Fig. 5b**). Specifically, the clearest result was that Fc–ephrin-B2–induced a significant decrease

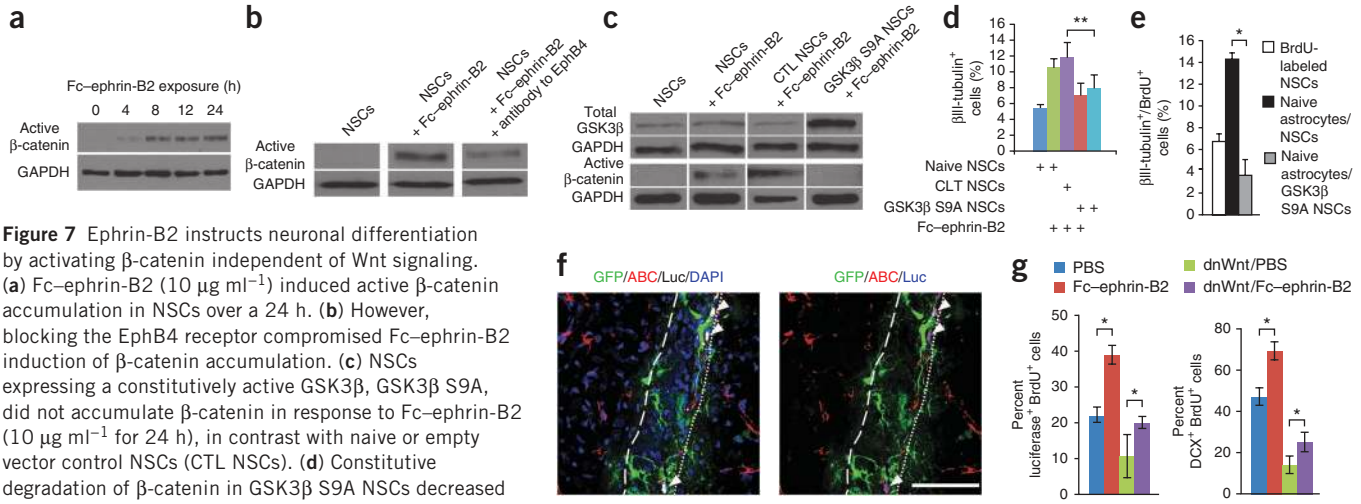

Figure 7 Ephrin-B2 instructs neuronal differentiation by activating β-catenin independent of Wnt signaling. (**a**) Fc–ephrin-B2 (10 μg ml^{-1}) induced active β-catenin accumulation in NSCs over a 24 h. (**b**) However, blocking the EphB4 receptor compromised Fc–ephrin-B2 induction of β-catenin accumulation. (**c**) NSCs expressing a constitutively active GSK3β, GSK3β S9A, did not accumulate β-catenin in response to Fc–ephrin-B2 (10 μg ml^{-1} for 24 h), in contrast with naive or empty vector control NSCs (CTL NSCs). (**d**) Constitutive degradation of β-catenin in GSK3β S9A NSCs decreased NSCs differentiation into βIII-tubulin$^+$ neurons in response to Fc–ephrin-B2 (10 μg ml^{-1}) versus empty vector control NSCs (CTL NSCs) ($n = 3$ experimental replicates). (**e**) The lack of β-catenin signaling in GSK3β S9A NSCs also nullified the proneuronal effect of hippocampus-derived, ephrin-B2–expressing astrocytes in co-culture ($n = 4$, experimental repeats). (**f**) In mice co-infected with Tcf-Luc and dnWnt-IRES-GFP constructs, cells in the SGZ still expressed active β-catenin (ABC) and luciferase (arrowheads; white in left panel) 24 h after Fc–ephrin-B2 injection. Scale bar represents 100 μm. (**g**) In hippocampi co-infected with Tcf-Luc and either dnWnt-IRES-GFP or IRES-GFP construct, then injected with Fc–ephrin-B2 or PBS, Fc–ephrin-B2 increased the percentage of SGZ BrdU$^+$ cells with active β-catenin signaling 24 h post-injection and the percentage of DCX$^+$ BrdU$^+$ cells by day 5 even with dnWnt present ($n = 4$ brains, 8 sections per brain). Thus, Ephrin-B2 activates β-catenin signaling and enhances adult neurogenesis independent of Wnt signaling. *$P < 0.01$ and **$P < 0.05$. Error bars represent ± s.d. Dotted and dashed lines indicate SGZ-hilus and GCL-MCL boundaries, respectively. Full length blots are shown in **Supplementary Figure 9**.

($P < 0.05$) in the percentage of single type 1 and single type 2a cells and a corresponding increase in the number of single neuronal cells (**Fig. 6i**). Likewise, there was a statistically significant decrease ($P < 0.05$) in the overall number of doublets containing a type 1 cell (1 + X) or a type 2a cell (2a + X), accompanied by an increase in the number of neuronal + neuronal doublets. These results are consistent with the interpretation that ephrin-B2 induced the conversion of type 1 and 2a cells toward more differentiated phenotypes, either with or without a cell division event. Finally, there was no change in the percentage of astrocyte-containing clonal β-gal$^+$ cell clusters, as anticipated because of the low levels of gliogenesis previously observed in this experimental procedure (**Supplementary Fig. 1**). In summary, these results indicate that ephrin-B2 signaling increases the commitment of type 1 and type 2a NSCs to a neuronal fate.

Wnt-independent induction of NSC neuronal differentiation

Activation of the canonical Wnt pathway elevates levels of β-catenin, followed by its nuclear translocation and association with Tcf/Lef transcription factors. Recently, this pathway was shown to regulate adult NSC differentiation by transcriptionally activating the proneural transcription factor NeuroD1 (refs. 23,37). In zebrafish paraxial mesoderm, ephrin-Eph forward signaling recruits β-catenin to adherens junctions[38], and EphB receptors are known transcriptional targets of β-catenin–Tcf signaling in stem cells in the mammalian gut[39]. However, to the best of our knowledge, ephrin-Eph signaling has not previously been shown to activate β-catenin signaling. Notably, we found that Fc–ephrin-B2 stimulation progressively increased the levels of intracellular active β-catenin in cultured NSCs over a 24-h period (**Fig. 7a**), initially detectable at 4 h and rising to maximal levels by 24 h. To determine whether this increased active β-catenin was mediated by EphB4, we pre-incubated NSCs with antibody to EphB4 before adding Fc–ephrin-B2. As observed in previous experiments (**Figs. 2c** and **4b**), EphB4 blockage decreased NSC responses to ephrin-B2 signaling and correspondingly limited the intracellular accumulation of active β-catenin (**Fig. 7b**).

In the canonical Wnt pathway, intracellular β-catenin levels are directly regulated by glycogen synthase kinase-3 beta (GSK3β), which phosphorylates β-catenin and thereby marks it for proteasomal degradation[40]. To determine whether elevated β-catenin activity is required for ephrin-B2's proneuronal effect, we generated NSCs expressing a constitutively active form of GSK3β (GSK3β S9A)[41]. Following stimulation with Fc–ephrin-B2, both naive NSCs and NSCs carrying a control empty retroviral vector exhibited increased levels of active β-catenin (**Fig. 7c**), consistent with prior results (**Fig. 7a**). However, GSK3β S9A NSCs were unable to accumulate β-catenin in response to ephrin-B2 signaling. Furthermore, unlike naive cells, GSK3β S9A NSCs resisted neuronal differentiation when stimulated with Fc–ephrin-B2 or co-cultured with ephrin-B2 expressing naive astrocytes, indicating that increased active β-catenin levels are required for ephrin-B2's proneuronal effect (**Fig. 7d,e**).

These results raise the possibility that ephrin-B2's pro-neuronal effect could involve Wnt ligand–mediated activation of β-catenin. To determine whether ephrin-B2 signaling indirectly activates β-catenin via upregulation of soluble Wnts *in vivo*, we used lentiviruses encoding a Tcf-Luciferase (Tcf-Luc) construct that reports β-catenin activity[42] and either a dominant-negative Wnt–IRES-GFP[23] (dnWnt-IRES-GFP) or IRES-GFP (control) cassette. We first confirmed that lentiviral-mediated expression of the soluble dnWnt by cultured NSCs significantly decreased luciferase reporter expression following incubation of the cells with Wnt3a ($P < 0.01$; **Supplementary Fig. 6**). β-catenin reporter vector, as well as vector expressing dnWnt or GFP alone, were then co-administered *in vivo*. After 2 weeks, mitotic cells in the rat hippocampi were labeled with BrdU, and Fc–ephrin-B2 or PBS was administered by intrahippocampal injection. After 24 h, in animals injected with Tcf-Luc and IRES-GFP constructs, Fc–ephrin-B2 increased the number of Luc$^+$ BrdU$^+$ cells, which also co-stained for active β-catenin, indicating that ephrin-B2 stimulates β-catenin signaling *in vivo* (**Fig. 7f,g**). Furthermore, administration of the dnWnt-IRES-GFP vector with the Tcf-Luc vector knocked down the number of Luc$^+$ BrdU$^+$ cells proportionally in the Fc–ephrin-B2– and

PBS-injected groups, indicating that Wnt signaling is active in the hippocampus, but that ephrin-B2 still stimulates β-catenin signaling even when Wnt is inhibited. Consistent with these results, dnWnt reduced the number of newborn neurons in both the Fc–ephrin-B2– and PBS-injected animals by day 5, but the former still showed a significantly higher number of DCX^+ $BrdU^+$ cells than the latter ($P < 0.05$; **Fig. 7g**). Thus, ephin-B2 signaling does not apparently activate β-catenin through a soluble Wnt intermediate, and it can increase adult neurogenesis in the absence of Wnt signaling.

Finally, in NSC cultures stimulated with Fc–ephrin-B2, we observed a significant increase in the transcription of both *Mash1* (*Ascl1*, $P < 0.001$) and *Neurod1* ($P = 0.001$), proneural transcription factors that are known to be involved in adult hippocampal neurogenesis[37,43] (**Supplementary Fig. 7a**,**b**). This mRNA upregulation presumably occurred in the subset of cells that underwent neuronal differentiation. Thus, our collective results strongly indicate that hippocampal astrocytes instruct neuronal differentiation of $EphB4^+$ NSCs through juxtacrine ephrin-B2–EphB4 forward signaling, which induces the expression of proneural transcription factors via a β-catenin–dependent and soluble Wnt–independent mechanism.

DISCUSSION

Stem cell niches present repertoires of signals that control cell maintenance, proliferation and differentiation. Recent studies have identified several factors that regulate cell maintenance and proliferation in the adult NSC niche; however, few cues have been found to induce differentiation. Furthermore, although numerous soluble cues have been found to regulate adult neurogenesis, cell-cell interactions in the niche have, in general, been less studied. We found that ephrin-B2 presented from hippocampal astrocytes activated β-catenin signaling in NSCs, upregulated the expression of key proneural transcription factors and instructed their neuronal differentiation (**Supplementary Fig. 8**).

Hippocampal astrocytes, but not astrocytes derived from non-neurogenic regions of the CNS, regulate neurogenesis[22], and recent expression profiling analyzed the differential expression of factors that underlie this activity[19]. However, ephrin-B2 was not represented on the Affymetrix chip used for this important comparative gene expression study, and cues dependent on cell-cell contact between the stem cells and hippocampal astrocytes have not been explored. The importance of ephrins and their receptors in axon guidance, neural tissue patterning and synapse formation is well established[24]; however, less is known about their role in regulating adult NSCs. Several studies have shown that ephrin-Eph signaling can affect NSC proliferation[31–33,44]; however, these studies did not address the potential for ephrins and Ephs to regulate stem cell differentiation in the brain. Our results therefore represent, to the best of our knowledge, the first case of ephrin-Eph family regulation of NSC neuronal lineage commitment in the adult CNS.

We found that endogenous ephrin-B2 was expressed by astrocytes in close proximity to adult NSCs, shRNA-mediated knockdown of the endogenous ephrin-B2 substantially lowered the fraction of newborn cells that become DCX^+ neuronal precursors, and exogenous addition of ephrin-B2 induced the conversion of type 1 and 2a NSCs toward type 2b precursors and, subsequently, neurons (**Figs. 2**, **5** and **6**). Furthermore, lineage tracing analysis revealed a decrease in single type 1 and type 2a cells and an increase in the number of single neuroblasts and neurons in the presence of ephrin-B2, as well as a decrease in the number of cell doublets containing a type 1 or 2a cell with a corresponding increase in the number of neuroblast and neuron doublets (**Fig. 6**). These results are consistent with ectopic ephrin-B2 inducing β-catenin signaling and upregulation of proneural transcription factors (**Fig. 7** and **Supplementary Fig. 7a**,**b**) to induce NSC differentiation independent of cell division. Collectively, our results indicate that juxtacrine signaling between astrocytes and NSCs provides a mechanism for the niche to locally control NSC differentiation. Prior results have investigated the importance of Notch and EphB2 signaling in modulating the properties of neighboring cells in the NSC niche[45] and the importance of Notch in maintaining type 1 NSCs[13,46]. Together, these results increasingly establish cell contact–dependent signaling as a critical mechanism for locally regulating multiple stages in adult neurogenesis.

Ephrin-Eph signaling is generally known to be bidirectional, such that the Eph-presenting cell can activate signaling in the ephrin ligand–expressing cell[24]. We found that adult NSCs upregulated ephrin-B2 and downregulated EphB4 expression following differentiation into astrocytes *in vitro*, yet retained EphB4 expression following neuronal differentiation (**Supplementary Fig. 2b**). Ephrin-Eph signal feedback from the differentiating NSCs to neighboring cells could therefore represent a mechanism for dynamically remodeling the signaling environment of the niche, analogous to GDF11-dependent negative feedback from neurons to neural progenitors in the olfactory epithelium[47] or EGF-dependent feedback from neural progenitors to neural stem cells in the SVZ[48]. In addition, ephrin and Eph expression dynamics could help to control cell differentiation following NSC symmetric or asymmetric division[8] and thereby contribute to maintaining or modulating the cellular composition of the niche. The potential of ephrin signaling in general to support self-renewing, asymmetric cell division, that is, to generate a stem cell and a differentiated progeny, is virtually unexplored. There has been only one report of ephrin-mediated regulation of asymmetric stem cell division, in the ascidian embryo[49].

Type 1 NSCs were depleted following ephrin-B2 administration (**Fig. 6**), indicating that they may be direct targets of this ligand's signaling. However, although some type 1 cells expressed levels of EphB4 detectable by immunostaining and upregulated β-catenin signaling following ephrin-B2 addition, nearly all of the type 2a cells did so, and additional work will be needed to determine whether the observed differentiation of type 1 cells in response to ephrin-B2 is direct and/or indirect. In addition, although ephrin-B2 knockdown did not affect cell proliferation (**Fig. 5d**) and ephrin-B2 protein administration did not affect the proliferation of genetically labeled, Nestin-expressing stem and progenitor cells (**Fig. 6** and **Supplementary Fig. 5**), ephrin-B2 addition did result in the expansion of cells pre-labeled with BrdU in the rat brain. It is conceivable that, in addition to its clear role in inducing the differentiation of NSCs at the expense of stem cell maintenance or self-renewing cell divisions (**Fig. 6**), ephrin-B2 could also modulate the expansion of later stage neuroblasts that are strongly labeled with BrdU, a possibility that could be explored in the future.

In summary, our findings suggest that ephrin-B2, a transmembrane factor known for its role in cell and tissue patterning, is an important regulator of adult hippocampal neurogenesis, the first known function of an Eph family protein in regulating neuronal lineage commitment of NSCs in the adult CNS. In addition, hippocampal astrocytes are the source of the ephrin-B2 signal, which further supports the emerging view that astroglia are active and essential regulators of an increasing number of adult CNS functions, including remodeling the neurogenic niche through local cellular interactions. Moreover, the discovery that ephrin-B2 signals through β-catenin adds further understanding to the interconnected and likely synergistic nature by which niche factors regulate adult neurogenesis. Finally, our findings may have future applications in modulating NSC function for treating brain injury and neurodegenerative disease.

METHODS

Methods and any associated references are available in the online version of the paper.

Note: Supplementary information is available in the online version of the paper.

ACKNOWLEDGMENTS

We thank R. Fletcher for his guidance in mouse breeding and genotyping. This research was supported by US National Institutes of Health grant EB007295, Lawrence Berkeley National Lab Laboratory Directed Research and Development grant 3668DS and California Institute of Regenerative Medicine training grant T1-00007.

AUTHOR CONTRIBUTIONS

C.P. designed and executed the initial *in vitro* ephrin ligand studies. R.S.A. performed *in vitro* immunocytochemistry and A.C. performed *in vivo* immunohistochemistry. R.S.A. designed all of the ephrin-B2 *in vivo* gain-of-function and loss-of-function experiments, and A.C. and J.B. equally assisted in conducting the experiments. RNAi vectors were designed by R.S.A. and K.-I.L., cloned by K.-I.L. and P.S., and R.S.A. validated vectors experimentally and conducted *in vitro* RNAi and co-culture experiments. A.C. validated the expression of shRNA vectors in hippocampal astrocytes. R.S.A. conducted mouse breeding and designed and conducted fate mapping experiments with substantial input and assistance from A.C. A.C. conducted clonal analysis experiments, designed and conducted all of the experiments related to *in vivo* β-catenin activity studies, and analyzed tissue sample from both fate mapping and β-catenin activity studies. A.C. and C.P., and to a lesser extent R.S.A., executed the ephrin-B2, GSK3β S9A, β-catenin, *Mash1* and *NeuroD1* mechanistic studies. R.S.A. and A.C. performed statistical analysis. A.C. illustrated **Supplementary Figure 8**. R.S.A. and D.S. wrote the manuscript, with substantial input from A.C. D.V.S. supervised all aspects of this work and M.B. provided important scientific input and feedback.

COMPETING FINANCIAL INTERESTS

The authors declare no competing financial interests.

Published online at http://www.nature.com/doifinder/10.1038/nn.3212.
Reprints and permissions information is available online at http://www.nature.com/reprints/index.html.

1. Eriksson, P.S. *et al.* Neurogenesis in the adult human hippocampus. *Nat. Med.* **4**, 1313–1317 (1998).
2. Lois, C. & Alvarez-Buylla, A. Long-distance neuronal migration in the adult mammalian brain. *Science* **264**, 1145–1148 (1994).
3. Spalding, K.L., Bhardwaj, R.D., Buchholz, B.A., Druid, H. & Frisén, J. Retrospective birth dating of cells in humans. *Cell* **122**, 133–143 (2005).
4. Manganas, L.N. *et al.* Magnetic resonance spectroscopy identifies neural progenitor cells in the live human brain. *Science* **318**, 980–985 (2007).
5. Jessberger, S. *et al.* Seizure-associated, aberrant neurogenesis in adult rats characterized with retrovirus-mediated cell labeling. *J. Neurosci.* **27**, 9400–9407 (2007).
6. Ekdahl, C.T., Claasen, J.-H., Bonde, S., Kokaia, Z. & Lindvall, O. Inflammation is detrimental for neurogenesis in adult brain. *Proc. Natl. Acad. Sci. USA* **100**, 13632–13637 (2003).
7. Tattersfield, A.S. *et al.* Neurogenesis in the striatum of the quinolinic acid lesion model of Huntington's disease. *Neuroscience* **127**, 319–332 (2004).
8. Suh, H. *et al. In vivo* fate analysis reveals the multipotent and self-renewal capacities of Sox2$^+$ neural stem cells in the adult hippocampus. *Cell Stem Cell* **1**, 515–528 (2007).
9. Suh, H., Deng, W. & Gage, F.H. Signaling in adult neurogenesis. *Annu. Rev. Cell Dev. Biol.* **25**, 253–275 (2009).
10. Bonaguidi, M.A. *et al. In vivo* clonal analysis reveals self-renewing and multipotent adult neural stem cell characteristics. *Cell* **145**, 1142–1155 (2011).
11. Mira, H. *et al.* Signaling through BMPR-IA regulates quiescence and long-term activity of neural stem cells in the adult hippocampus. *Cell Stem Cell* **7**, 78–89 (2010).
12. Ehm, O. *et al.* RBPJ-dependent signaling is essential for long-term maintenance of neural stem cells in the adult hippocampus. *J. Neurosci.* **30**, 13794–13807 (2010).
13. Lugert, S. *et al.* Quiescent and active hippocampal neural stem cells with distinct morphologies respond selectively to physiological and pathological stimuli and aging. *Cell Stem Cell* **6**, 445–456 (2010).
14. Lai, K., Kaspar, B.K., Gage, F.H. & Schaffer, D.V. Sonic hedgehog regulates adult neural progenitor proliferation *in vitro* and *in vivo*. *Nat. Neurosci.* **6**, 21–27 (2003).
15. Jin, K. *et al.* Neurogenesis and aging: FGF-2 and HB-EGF restore neurogenesis in hippocampus and subventricular zone of aged mice. *Aging Cell* **2**, 175–183 (2003).
16. Cao, L. *et al.* VEGF links hippocampal activity with neurogenesis, learning and memory. *Nat. Genet.* **36**, 827–835 (2004).
17. Qu, Q. *et al.* Orphan nuclear receptor TLX activates Wnt/beta-catenin signaling to stimulate neural stem cell proliferation and self-renewal. *Nat. Cell Biol.* **12**, 31–40 (2010).
18. Gage, F.H. *et al.* Survival and differentiation of adult neuronal progenitor cells transplanted to the adult brain. *Proc. Natl. Acad. Sci. USA* **92**, 11879–11883 (1995).
19. Barkho, B.Z. *et al.* Identification of astrocyte-expressed factors that modulate neural stem/progenitor cell differentiation. *Stem Cells Dev.* **15**, 407–421 (2006).
20. Tozuka, Y., Fukuda, S., Namba, T., Seki, T. & Hisatsune, T. GABAergic excitation promotes neuronal differentiation in adult hippocampal progenitor cells. *Neuron* **47**, 803–815 (2005).
21. Jacobs, S. *et al.* Retinoic acid is required early during adult neurogenesis in the dentate gyrus. *Proc. Natl. Acad. Sci. USA* **103**, 3902–3907 (2006).
22. Song, H., Stevens, C.F. & Gage, F.H. Astroglia induce neurogenesis from adult neural stem cells. *Nature* **417**, 39–44 (2002).
23. Lie, D.-C. Wnt signaling regulates adult hippocampal neurogenesis. *Nature* **437**, 1370–1375 (2005).
24. Pasquale, E.B. Eph receptor signaling casts a wide net on cell behaviour. *Nat. Rev. Mol. Cell Biol.* **6**, 462–475 (2005).
25. Knöll, B. & Drescher, U. Ephrin-As as receptors in topographic projections. *Trends Neurosci.* **25**, 145–149 (2002).
26. Martínez, A. & Soriano, E. Functions of ephrin/Eph interactions in the development of the nervous system: emphasis on the hippocampal system. *Brain Res. Brain Res. Rev.* **49**, 211–226 (2005).
27. Xu, N.-J., Sun, S., Gibson, J.R. & Henkemeyer, M. A dual shaping mechanism for postsynaptic ephrin-B3 as a receptor that sculpts dendrites and synapses. *Nat. Neurosci.* **14**, 1421–1429 (2011).
28. Aoki, M., Yamashita, T. & Tohyama, M. EphA receptors direct the differentiation of mammalian neural precursor cells through a mitogen-activated protein kinase–dependent pathway. *J. Biol. Chem.* **279**, 32643–32650 (2004).
29. del Valle, K., Theus, M.H., Bethea, J.R., Liebl, D.J. & Ricard, J. Neural progenitors proliferation is inhibited by EphB3 in the developing subventricular zone. *Int. J. Dev. Neurosci.* **29**, 9–14 (2011).
30. Conover, J.C. *et al.* Disruption of Eph/ephrin signaling affects migration and proliferation in the adult subventricular zone. *Nat. Neurosci.* **3**, 1091–1097 (2000).
31. Holmberg, J. *et al.* Ephrin-A2 reverse signaling negatively regulates neural progenitor proliferation and neurogenesis. *Genes Dev.* **19**, 462–471 (2005).
32. Chumley, M.J., Catchpole, T., Silvany, R.E., Kernie, S.G. & Henkemeyer, M. EphB receptors regulate stem/progenitor cell proliferation, migration, and polarity during hippocampal neurogenesis. *J. Neurosci.* **27**, 13481–13490 (2007).
33. Hara, Y., Nomura, T., Yoshizaki, K., Frisén, J. & Osumi, N. Impaired hippocampal neurogenesis and vascular formation in ephrin-A5–deficient mice. *Stem Cells* **28**, 974–983 (2010).
34. Davis, S. *et al.* Ligands for EPH-related receptor tyrosine kinases that require membrane attachment or clustering for activity. *Science* **266**, 816–819 (1994).
35. Battiste, J. *et al.* Ascl1 defines sequentially generated lineage-restricted neuronal and oligodendrocyte precursor cells in the spinal cord. *Development* **134**, 285–293 (2007).
36. Soriano, P. Generalized lacZ expression with the ROSA26 Cre reporter strain. *Nat. Genet.* **21**, 70–71 (1999).
37. Kuwabara, T. *et al.* Wnt-mediated activation of NeuroD1 and retro-elements during adult neurogenesis. *Nat. Neurosci.* **12**, 1097–1105 (2009).
38. Barrios, A. *et al.* Eph/Ephrin signaling regulates the mesenchymal-to-epithelial transition of the paraxial mesoderm during somite morphogenesis. *Curr. Biol.* **13**, 1571–1582 (2003).
39. Batlle, E. *et al.* Beta-catenin and TCF mediate cell positioning in the intestinal epithelium by controlling the expression of EphB/ephrinB. *Cell* **111**, 251–263 (2002).
40. Kim, W.-Y. *et al.* GSK-3 is a master regulator of neural progenitor homeostasis. *Nat. Neurosci.* **12**, 1390–1397 (2009).
41. Stambolic, V. & Woodgett, J.R. Mitogen inactivation of glycogen synthase kinase-3 beta in intact cells via serine 9 phosphorylation. *Biochem. J.* **303**, 701–704 (1994).
42. Fuerer, C. & Nusse, R. Lentiviral vectors to probe and manipulate the Wnt signaling pathway. *PLoS ONE* **5**, e9370 (2010).
43. Elmi, M. *et al.* TLX activates MASH1 for induction of neuronal lineage commitment of adult hippocampal neuroprogenitors. *Mol. Cell. Neurosci.* **45**, 121–131 (2010).
44. Jiao, J.-W., Feldheim, D.A. & Chen, D.F. Ephrins as negative regulators of adult neurogenesis in diverse regions of the central nervous system. *Proc. Natl. Acad. Sci. USA* **105**, 8778–8783 (2008).
45. Nomura, T., Göritz, C., Catchpole, T., Henkemeyer, M. & Frisén, J. EphB signaling controls lineage plasticity of adult neural stem cell niche cells. *Cell Stem Cell* **7**, 730–743 (2010).
46. Ables, J.L. *et al.* Notch1 is required for maintenance of the reservoir of adult hippocampal stem cells. *J. Neurosci.* **30**, 10484–10492 (2010).
47. Wu, H.-H. *et al.* Autoregulation of neurogenesis by GDF11. *Neuron* **37**, 197–207 (2003).
48. Aguirre, A., Rubio, M.E. & Gallo, V. Notch and EGFR pathway interaction regulates neural stem cell number and self-renewal. *Nature* **467**, 323–327 (2010).
49. Picco, V., Hudson, C. & Yasuo, H. Ephrin-Eph signalling drives the asymmetric division of notochord/neural precursors in Ciona embryos. *Development* **134**, 1491–1497 (2007).

ONLINE METHODS

Cell culture. NSCs isolated from the hippocampi of 6-week-old female Fisher 344 rats (Charles River) were cultured as previously described[14] on poly-ornithine/laminin-coated plates in DMEM/F12 medium (Life Technologies) containing N2 supplement (Life Technologies) and 20 ng ml^{-1} FGF-2 (PeproTech), with subculturing on reaching 80% confluency using Accutase (Phoenix Flow Systems). To induce differentiation, we cultured NSCs for 5 d in DMEM/F12/N2 medium supplemented with 2% fetal bovine serum (vol/vol, Life Technologies) and 1 μM retinoic acid (Biomol). Rat hippocampal astrocytes were isolated from Fisher 344 rats (Charles River) as previously described[22] and cultured on poly-ornithine/laminin-coated plates in DMEM/F12/N2 supplemented with 10% fetal bovine serum, with subculture on reaching 90% confluency using Trypsin EDTA (Mediatech).

Fc–ephrin-B2 synthesis and differentiation assays. To generate Fc–ephrin-B2, we incubated mouse ephrin-B2/Fc (Sigma Aldrich) at a 9:1 ratio (wt/wt) with a goat antibody to human IgG Fc (Jackson ImmunoResearch, cat. #109-005-098) for 90 min at 4 °C before immediate use. To differentiate NSC *in vitro*, we seeded eight-well chamber slides with 5×10^4 cells per well in standard culture medium containing 20 ng ml^{-1} FGF-2. The next day, the medium was replaced with DMEM/F12 containing 0.5 ng ml^{-1} FGF-2 and various concentrations of Fc–ephrin-B2. Differentiation experiments were performed over a 4-d period with a 50% media change daily. Then, the cells were fixed using 4% paraformaldehyde (PFA, Sigma Aldrich) and stained using standard protocols (see below). To test the effect of Eph receptor blocking, we pre-incubated NSCs with goat antibodies to EphB4 or EphB2 (1:50, Santa Cruz Biotechnology, cat. #sc-7285 and #sc-1763) for 30 min before addition of Fc–ephrin-B2 ligands.

Lentiviral and retroviral vector construction. DNA cassettes containing either human or mouse U6 promoter–driven expression of candidate shRNAs to rat *Efnb2* (Gene ID: 306636) were constructed by PCR. The forward primer containing a *Pac*I site for cloning and the reverse primer containing the entire shRNA sequence were used to amplify the U6 promoter from template plasmids pFhU6ABCgUGW (unpublished observation) or pmU6 pro. PCR was performed using Phusion high-fidelity polymerase (Finnzymes) under the following conditions: pre-incubation at 98 °C for 2 min, 30 cycles, with 1 cycle consisting of 12 s at 98 °C, 30 s at 55–65 °C, and 15–25 s at 72 °C, and a final extension step of 2 min at 72 °C. The U6 sense primers were sense_hU6 (5′-AACAATTAATTAAAAGGTCGGGCAGGAAGAGGGCCTATT-3′) and sense_mU6 (5′-AACAATTAATTAAATCCGACGCCGCCATCTCTAGGCC-3′). For a listing of the shRNA encoding antisense primers, see **Supplementary Table 1**. In parallel, a control shRNA cassette against *lacZ* was constructed[50] analogously, using pBS U6 shRNA β-gal as the template and with primers listed in **Supplementary Table 1**. All PCR products were digested with *Pac*I and cloned into the pFUGW lentiviral vector[51] upstream of the human *UBC* promoter and eGFP. pCLGPIT–GSK3β S9A, encoding a constitutively active form of GSK3β (a gift of A. Fritz and S. Agrawal, University of California, Berkeley), was constructed by amplifying the GSK3β sequence from rat NSC cDNA, inserting it into pCLGPIT, and subjecting the plasmid to a site-directed mutagenesis to introduce the S9A mutation. Lentiviral and retroviral vectors were packaged using standard methods as described elsewhere[52,53]. Lastly, to validate functionality of the *Efnb2* shRNA vectors, the mouse *Gfap* promoter[54], as well as the human *GFAP* promoter[55], was cloned into the digested pFUGW vector, replacing the *UBC* promoter upstream of eGFP.

Ephrin-B2 RNAi co-cultures. To select effective shRNA sequences targeting *Efnb2*, we transduced hippocampus-derived astrocytes with lentivirus encoding trial shRNA sequences at a multiplicity of infection (MOI) of 3 and cultured them for 4 d. RNA isolated from astrocyte cultures was analyzed for *Efnb2* expression using QPCR (see below and **Supplementary Fig. 3**). For co-culture assays, hippocampus-derived astrocytes were transduced with lentivirus encoding shRNA sequences at an MOI of 3 and cultured for 2 d before a 3-d incubation in medium containing 20 μM cytosine arabinoside (AraC, Sigma Aldrich) to deplete rapidly dividing astrocytes. Cells were then returned to standard medium for 24 h before being subcultured onto eight-well chamber slides at a density of 70,000 cells per cm^2. NSCs were transduced with retrovirus encoding either pCLGPIT or pCLGPIT–GSK3β S9A at an MOI of 1 and cultured for 2 d before a 96-h selection period in medium containing 1 μg ml^{-1} puromycin (Sigma Aldrich). Next, NSCs were incubated in standard media containing 25 μM BrdU (Sigma Aldrich) for 48 h. The BrdU-labeled NSCs were then seeded on top of a monolayer of astrocytes in eight-well chamber slides at a density of 70,000 cells per cm^2 in medium lacking FGF-2. Co-cultures were maintained for 6 d before fixation and analysis by immunocytochemistry.

***In vivo* gain and loss of function studies.** All animal protocols were approved by the Institutional Animal Care and Use Committee of the University of California Berkeley. We intraperitoneally injected 8-week-old adult female Fisher 344 rats daily with BrdU (50 mg per kg of body weight, Sigma Aldrich) dissolved in saline to label mitotic cells, as previously described[14]. In Fc–ephrin-B2 studies, rats were anesthetized before 3-μl bilateral intrahippocampal stereotaxic injections of either PBS (Life Technologies), ephrin-B2 (14 μg ml^{-1}), antibody to Fc (126 μg ml^{-1}) or Fc–ephrin-B2 (140 μg ml^{-1}) in PBS. The injection coordinates were −3.5 mm anterior-posterior and ±2.5 mm mediolateral relative to bregma, and −3.0 mm dorsoventral relative to dura (refer to **Fig. 3a** for injection time course). Unbiased stereology (Zeiss Axio Imager, software by MicroBrightfield) using the optical fractionator method was performed on eight evenly distributed sections from each rat to estimate the total number of relevant cells throughout the entire hippocampus. In RNAi studies, rats received bilateral intrahippocampal injections of 3 μl of lentiviral solutions in PBS on day −19. The injection coordinates with respect to bregma were −3.5 mm anteriorposterior, −3.5 mm dorsoventral (that is, from the dura) and ± 2.0 mm mediolateral (refer to **Fig. 5a** for injection time course). Unbiased stereology was performed on eight GFP$^+$ hippocampal sections from each rat, and the number of selected cells was normalized by the volume of hippocampal tissue analyzed.

***In vivo* fate mapping.** *Nestin-CreER^{T2}* mice[35] (a kind gift from A. Eisch, University of Texas Southwestern) and *R26-stop$^{loxP/loxP}$-lacZ* mice[36] (a kind gift from J. Ngai, University of California Berkeley), both having a 100% C57/Bl6 background, were crossbreed twice to generate a homozygous *Nestin-CreER^{T2}; R26-stop$^{loxP/loxP}$-lacZ* mosue strain. Geneotyping was performed using the following primers: Cre-F (5′-ACCAGCCAGCTATCAACTCG-3′), Cre-R (5′- TTACATTGGTCCAGCCACC-3′), 200bp; lacZ-F (5′-GTCAATCCGCCGTTTGTTCCCACG-3′), lacZ-R (5′-CCAGTACAGCGCGGCTGAAATCAT-3′), 400 bp; wtRosa-F (5′-GGAGCGGGAGAAATGGATATG-3′), wtRosa-R (5′- AAAGTCGCTCTGAGTTGTTAT-3′), 600bp. To induce recombination and label mitotic cells, 5-week-old *Nestin-CreER^{T2}; R26-stop$^{loxP/loxP}$-lacZ* mice were administered 180 mg per kg tamoxifen (intraperitoneal, Sigma Aldrich) dissolved in corn oil and 50 mg per kg BrdU daily for 3 d before intrahippocampal injections of experimental solutions. We then administered 1 μl of antibody to Fc (126 μg ml^{-1}) and Fc–ephrin-B2 (140 μg ml^{-1}) in PBS at −2.12 mm anteriorposterior, −1.55 mm dorsoventral (from dura), and ±1.5 mm mediolateral with respect to the bregma. Pre-determined groups of mice (balanced in male-to-female ratio) were killed on days 0 (sham), 5 and 14, and tissue collection and histology were performed.

***In vitro* validation of β-catenin reporter and dnWnt vectors.** NSCs were co-infected with 7xTcf-FFluc[42] (Tcf-Luc) and either LV-dnWnt-IRES-GFP[23] or LV-GFP and expanded in culture. After a 24-h pulse with Wnt3a (200 ng ml^{-1}), cell lysates were collected and analyzed using Luc-Screen Extended-Glow Luciferase Reporter Gene Assay System (Applied Biosystems) and a TD-20/20 luminometer (Turner BioSystems) to determine the relative level of β-catenin activation.

***In vivo* β-catenin activation and Wnt-independent neurogenesis.** We injected 8-week-old adult female Fisher 344 rats with a mixture of half 7xTcf-FFluc[42] (Tcf-Luc) and half LV-dnWnt-IRES-GFP[23] or LV-GFP (kind gifts from F. Gage, Salk Institute) lentiviral vectors on day −17 (bilateral, intrahippocampal, stereotaxic, 3 μl). Starting on day −3, animals were intraperitoneally injected with BrdU (50 mg per kg) for 3 d before subsequent bilateral intrahippocampal stereotaxic injections of 3 μl of either Fc–ephrin-B2 (140 μg ml^{-1}) or PBS on day 0. The injection coordinates with respect to the bregma were −3.5 mm anteriorposterior, −3.4 mm dorsoventral (from dura), and ±1.8 mm mediolateral. Half of the rats were killed on day 1 and half were killed on day 5 before brains were processed for histology and analyzed by stereology.

Immunostaining and imaging. Cells cultures were fixed with 4% PFA for 10 min, blocked for 1 h with 5% donkey serum (vol/vol, Sigma), permeabilized

with 0.3% Triton X-100 (vol/vol, Calbiochem), and incubated for 48 h with combinations of the following primary antibodies: mouse antibody to nestin (1:1,000, BD Pharmingen, cat. #556309), rabbit antibody to GFAP (1:250, Abcam, cat. #ab7260), rabbit antibody to βIII-tubulin (1:250, Sigma, cat. #T8578) and rabbit antibody to MBP (1:100, Abcam, cat. #ab7349). Appropriate Cy3-, Cy5- or Alexa Fluor 488–conjugated secondary antibodies were used to detect primary antibodies (1:250, Jackson Immunoresearch; 1:250, Molecular Probes). TO-PRO-3 (10 μM, Life Technologies, cat. #T3605) or DAPI were used as the nuclear counterstain.

Animals were perfused with 4% PFA (wt/vol, Sigma), and brain tissue was extracted, stored in fixative for 24 h and allowed to settle in a 30% sucrose solution. Brains were coronally sectioned and immunostained using previously published protocols[14]. For primary antibodies, we used mouse antibody to BrdU (1:100, Roche, cat. #11170376001), mouse antibody to NeuN (1:100, Millipore, cat. #MAB377), rat antibody to BrdU (1:100, Abcam, cat. #ab6326), goat antibody to doublecortin (1:50, Santa Cruz Biotechnology, cat. #sc-8066), rabbit antibody to GFAP (1:1,000, Abcam, cat. #ab7260), guinea pig antibody to doublecortin (1:1,000, Millipore, cat. #AB2253), goat antibody to ephrin-B2 (1:10, R&D Systems, cat. #AF496), rabbit antibody to Sox2 (1:250, Millipore, cat. #AB5603), goat antibody to EphB4 (1:50, Santa Cruz, cat. #sc-7285), mouse antibody to GFAP (1:2,000, Advanced Immunochemical, cat. #8-GFAP-h), rabbit antibody to GFP (1:2000, Life Technologies, cat. #A-11122), goat antibody to GFP (1:200, Abcam, cat. #ab6673), and rabbit antibody to β-gal (gift from J. Ngai, University of California Berkeley). Appropriate Cy3-, Cy5- or Alexa Fluor 488–conjugated secondary antibodies (1:125, Jackson Immunoresearch; affinity-purified whole IgG with minimal cross-reactivity, 1:250, Life Technologies, Alexa Fluor-conjugated secondary antibodies) were used. For sections stained with rat antibody to BrdU, biotin-conjugated antibody to rat IgG (1:250, Jackson Immunoresearch, cat. #712-065-150) was used as the secondary, which was then washed and incubated with Cy3-conjugated streptavidin (1:1,000, Jackson Immunoresearch, cat. #016-160-084) for 2 h to amplify the signal. DAPI (50 μg ml^{-1}, Invitrogen) was used as a nuclear counterstain. Sections were mounted on glass slides and analyzed using the optical fractionator method in unbiased stereological microscopy (Zeiss Axio Imager, software by MicroBrightfield) and/or imaged with either a Leica Microsystems confocal microscope or a Zeiss 510 Meta UV/VIS confocal microscope located in the CNR Biological Imagining Facility at the University of California Berkeley.

Western blotting. NSCs were seeded at 2.5 × 10^5 cells per well in a six-well culture dish in standard culture medium containing 0.1 μg ml^{-1} FGF2. The following day, 10 μg ml^{-1} Fc–ephrin-B2 was added using a 50% media change. To test the effect of inhibition of the EphB4 receptor, NSCs were pre-incubated with goat antibody to EphB4 (1:50, Santa Cruz Biotechnology) for 30 min before addition of Fc–ephrin-B2. Cell lysates were collected at various time intervals (0–24 h after Fc–ephrin-B2 addition) and western blotted as previously described[56]. On nitrocellulose membranes, proteins were labeled using mouse antibody to active β-catenin (1:500, Millipore, cat. #05-665) and rabbit antibody to total GSK-3β (1:1,000, Cell Signaling, cat. #9315) in combination with the appropriate horseradish peroxidase–conjugated secondary antibody (1:10,000, Pierce, cat. #32430 and #32460). SuperSignal West Dura Extended Duration Substrate (Pierce) was used to detect the protein bands, and after film development (Kodak Film Processor 5000RA), membranes were stripped and re-probed with rabbit antibody to GAPDH (1:2,500, Abcam, cat. #ab9485).

RNA isolation and QPCR. RNA samples were isolated using standard Trizol (Life Technologies) collection and ethanol precipitation. RNA samples were quantified using a NanoDrop Spectrophotomer ND-1000 (NanoDrop Technologies), and equivalent amounts of RNA were added to QPCR reactions. QPCR was performed to probe for expression of nestin, GFAP, βIII-tubulin and 18S mRNA using previously described protocols[57]. For analysis of ephrin-B2 mRNA levels, QPCR was performed using a Taqman Gene Expression Assay (Applied Biosystems) for *Efnb2* (#Rn01215895_m1) and for eukaryotic *18S* (#803026). All reactions were performed using a BioRad IQ5 Multicolor Real-Time Detection System, and target mRNA expression levels were normalized according to levels of 18S.

Statistical analysis. Statistical significance of the results was determined using an ANOVA and multiple means comparison function (Tukey-Kramer analysis) in Matlab (Mathworks). Data are represented as means ± s.d.

50. Qin, X.F., An, D.S., Chen, I.S.Y. & Baltimore, D. Inhibiting HIV-1 infection in human T cells by lentiviral-mediated delivery of small interfering RNA against CCR5. *Proc. Natl. Acad. Sci. USA* **100**, 183–188 (2003).
51. Lois, C., Hong, E.J., Pease, S., Brown, E.J. & Baltimore, D. Germline transmission and tissue-specific expression of transgenes delivered by lentiviral vectors. *Science* **295**, 868–872 (2002).
52. Yu, J.H. & Schaffer, D.V. Selection of novel vesicular stomatitis virus glycoprotein variants from a peptide insertion library for enhanced purification of retroviral and lentiviral vectors. *J. Virol.* **80**, 3285–3292 (2006).
53. Lim, K.-I., Klimczak, R., Yu, J.H. & Schaffer, D.V. Specific insertions of zinc finger domains into Gag-Pol yield engineered retroviral vectors with selective integration properties. *Proc. Natl. Acad. Sci. USA* **107**, 12475–12480 (2010).
54. Greenberg, K.P., Geller, S.F., Schaffer, D.V. & Flannery, J.G. Targeted transgene expression in muller glia of normal and diseased retinas using lentiviral vectors. *Invest. Ophthalmol. Vis. Sci.* **48**, 1844–1852 (2007).
55. Lawlor, P.A., Bland, R.J., Mouravlev, A., Young, D. & During, M.J. Efficient gene delivery and selective transduction of glial cells in the mammalian brain by AAV serotypes isolated from nonhuman primates. *Mol. Ther.* **17**, 1692–1702 (2009).
56. Peltier, J., O'Neill, A. & Schaffer, D.V. PI3K/Akt and CREB regulate adult neural hippocampal progenitor proliferation and differentiation. *Dev. Neurobiol.* **67**, 1348–1361 (2007).
57. Peltier, J., Agrawal, S., Robertson, M.J. & Schaffer, D.V. *In vitro* culture and analysis of adult hippocampal neural progenitors. *Methods Mol. Biol.* **621**, 65–87 (2010).

doi:10.1038/nn.3212